Phys. Status Solidi C **14,** No. 7, 1700094 (2017) / **DOI** 10.1002/pssc.201700094

physica status solidi c
www.pss-c.com
current topics in solid state physics

Impact of damages in monocrystalline n-Si on material photosensitivity

Marina Tigishvili*,[1], Nina Khuchua,[2], Nodar Gapishvili[1], Tatiana Sakharova[1], Nugzar Dolidze[1], Zurab Jibuti[1], Giorgi Peradze[1], and Revaz Melkadze[2]**

[1] Institute of Micro- and Nanoelectronics, 13, Chavchavadze ave., Tbilisi 0179, Georgia
[2] Institute of Applied Semiconductor Technology, Iv.Javakhishvili Tbilisi State University, 13, Chavchavadze ave., Tbilisi 0179, Georgia

Received 27 February 2017, accepted 10 May 2017
Published online 26 May 2017

Keywords B^+ implantation, damaged layer, deep-level defects, IR photosensitivity, monocrystalline silicon

* Corresponding author: email tigishvilimarina@gmail.com, Phone: +995 32 222 06 44, Fax: +995 32 222 06 26
** email ninakhuchua@mail.ru, Phone: +995 32 222 06 26, Fax: +995 32 222 06 26

The optical and electrical characteristics of p–n photodiodes based on monocrystalline n-Si (wafers with $\rho = 70$ and 10 Ohm · cm and SOI) implanted with B^+ in the dose range of 1×10^{14}–1×10^{15} cm^{-2} and annealed at 900 °C (20 min) are studied. The p–n structures exhibit photosensitivity in the short-wavelength infrared region (SWIR) with different maximum intensities depending on dose and n-Si resistivity. Leakage currents are also dose-dependent. The character of the SOI spectra is somewhat different. The optical and electrical properties of p–n photodiodes are described in terms of formation of extended defects with deep levels in the bandgap appearing after B implantation and annealing of n-Si. The importance of the damaged surface layer in the starting material for the observed effects is confirmed experimentally. The relation of the SWIR photoresponse intensity to the content of C and O gettered to the p–n structure surface is revealed. The innovative aspects of technology application are discussed.

1 General Structural disorders and the presence (introduction) of impurities in a semiconductor significantly affect its electrical and optical properties, and hence the performance of relevant devices. Under external impacts, the formation of new defects in the material are observed. Such impacts become very important regarding the optical properties for silicon which is transparent to wavelengths beyond 1.1 μm. For example, structural and optical properties of Si can be modified by external actions such as electronic pulse treatment which shifts the self-absorption edge of Si to 1.33 μm [1], or boron implantation into n-Si which evokes a photoresponse within 1.5–2.2 μm [2–4]. With a high degree of probability it can be stated that in the first case, this might be due to a change in the band structure of silicon, whereas in the latter, defects with deep-levels (DL) in the material appear.

These studies are a continuation of previous work on the influence of the technology of boron implantation of monocrystalline n-Si on optical and other properties of the material.

Though boron is one of the most widely used and studied impurities in silicon, many unresolved issues remain concerning the nature of the defects formed and transformed under various conditions of implantation and annealing [5].

Even less information exists on the mechanism of the influence of various damages on optical properties of B implanted n-type monocrystalline silicon. As electroluminescence spectra are still discussed in many papers, absorption/photosensitivity spectra are studied very poorly and are rarely related to any type of defects [5–7].

Therefore, any new data on optical properties, and in particular IR photosensitivity of p-n Si structures as well as the possibility to obtain a deeper insight into the relationship between defect formation and these properties, is surely of scientific and practical interest.

In this study, B^+ implantation was performed in the range of 1×10^{14}–1×10^{15} cm^{-2}, and annealing at 900 °C (20 min). The lower dose limit was chosen according to the well-known conception that for the formation of residual extended defects in Si "threshold conditions", have to be applied. This means that for 10–100 keV the accumulation of a critical concentration of point defects requires a dose of at least 1×10^{14} cm^{-2} [8–10].

It should also be taken into account that, for doses beyond a critical level and for annealing temperatures over 700 °C, point radiation defects and clusters are annealed/transformed into extended defects (rod-like, dislocation loops, etc.) [11, 12].

We used a dose of $1 \times 10^{13}\,cm^{-2}$ at which the photoresponse should not be observed to ascertain whether the damaged surface layer in the starting material has any influence on the formation of extended defects determining the optical properties of the diodes.

Finally, of interest was to supplement the data of [2] with the information on a possible role of most "relevant" impurities such as carbon and oxygen gettered at the silicon surface [12, 13].

To explain the obtained results, the following notions are used:

- formation of extended defects introducing DL with different occupancy into the bandgap depending on the implantation and annealing regimes;
- a possibility of abnormally deep penetration of defects induced by ion implantation and their appearance beyond the p-n junction with allowance for the long-range effect model (see, e.g., Ref. [14]);
- the decisive role of the damaged surface layer in the starting material;
- participation of the C and O impurities gettered at the structure surface due to boron implantation in the formation of defects affecting the photoresponse.

The innovative aspects of technology application are considered.

2 Material, technology, methods of measurement p–n Si structures were formed by ion implantation (implanter Vesuvii 3M) of boron with different doses in the range of 1×10^{14}–$1 \times 10^{15}\,cm^{-2}$ and an acceleration energy of 50 keV. Post-implantation annealing was carried out mainly in a steady-state regime at the temperature of 900 °C (20 min). For comparison, some samples were subjected to pulse photon annealing in the original pulse photon radiation system. The design of the system allows illumination of the specimen surface with UV light, and the back side with a halogen lamp.

Figure 1 shows a schematic view of the processed p–n structures of two types.

In the case of Fig. 1a, (100) n-Si monocrystalline substrates with resistivity of about 70 or 10 Ohm · cm and thickness of 250 μm (University Wafer, USA) were used as a starting material. According to Fig. 1b, the specimen were SOI structures with the working layer of monocrystalline n-Si with a thickness of 2 μm and resistivity up to 30 Ohm · cm. The dielectric layer was also 2 μm thick (manufacturer – Ultrasil Corporation, USA). After B^+ implantation and annealing, a metal composition Ti/Pt/Au with a thickness of 100, 100, and 1000 Å, respectively, or Ti/Au was deposited (through a mask or by lift-off photolithography) in the Temescal setup. The alloying was performed in the 210 HEATPULSE system at 350 °C (15 s).

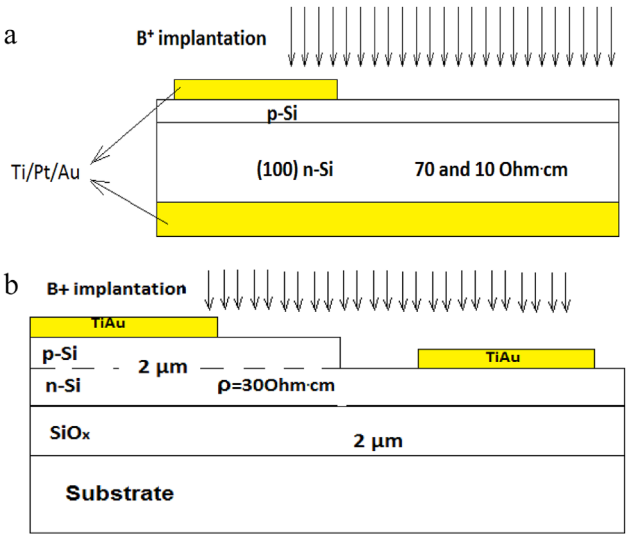

Figure 1 Schematic view of the p–n structures after processing: a) on n-Si wafers with different resistivity (Si70) and (Si10); b) on SOI.

First type structures (Fig. 1a) had a continuous lower contact, and a point contact for the p-type layer. In the SOI structure (Fig. 1b), both contacts were formed on the active layer. The mesa structure was obtained by wet etching in a fluorine-containing solution using the acid-resistant photoresist mask.

The photosensitivity of the samples in the spectral range of 1.0–2.5 μm was measured by standard methods on a MDR-2 monochromator with IR optical filters.

The integral photoresponse of the samples in different spectral regions within 0.2–4.1 μm was studied using the original setup and the system of optical filters. As a source of illumination, mercury and halogen incandescent lamps were used.

In the first case, the photo-emf and in the second case short-circuit current is measured.

The elemental content (weight percent) of the structures to a depth of 1 μm was studied on a YEOL ISU-6510LV scanning electron microscope (SEM). This method of sensitivity 0.01% and less was used to determine the C and O composition in Si averaged over the sample surface.

3 Experimental results and discussion Figure 2 shows the diode characteristics typical of the studied structures, implanted with a dose of $4 \times 10^{14}\,cm^{-2}$ and annealed at 900 °C (20 min).

The reverse branch in Fig. 2b starts bending already at $U = -4$ V .

Figure 3 illustrates the behavior patterns of leakage currents at different implantation doses for p–n diodes at the voltage of −2 V (the value frequently used in practice). Of particular interest are the data for the Si70 samples: up to the

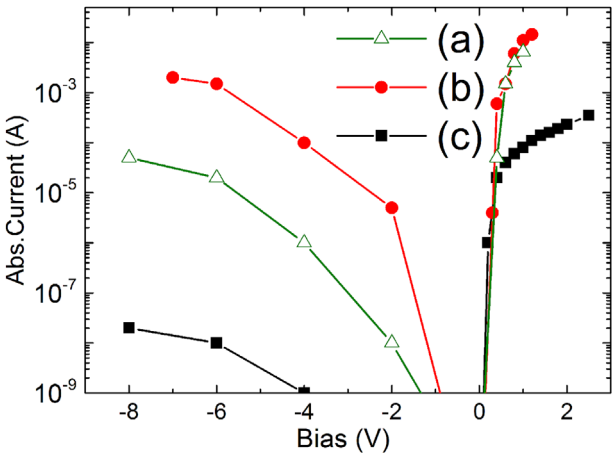

Figure 2 *I–V* characteristics of the p-n diodes: a) Si70; b) Si10 c) SOI.

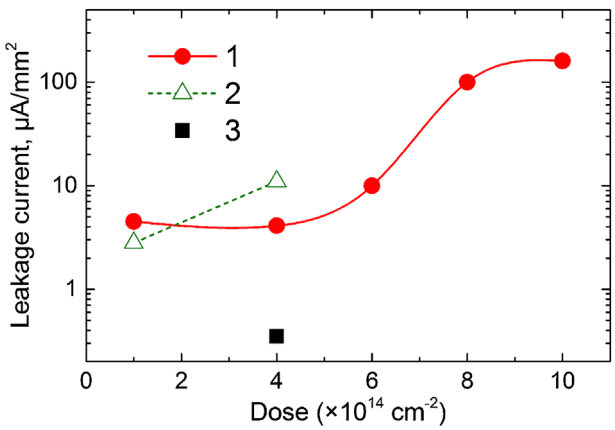

Figure 3 Dependence of the average values of the leakage current density at −2 V on the implantation dose for different samples: 1 – Si70, without mesa-etching; 2 – Si10; 3 – SOI (both – with mesa-etching).

dose of 6×10^{14} cm^{-2} no significant change in the leakage currents is observed, while the change at higher doses is more than two orders of magnitude. Of interest is the fact that at annealing of the samples implanted with 1×10^{15} cm^{-2}, in the stationary regime of 1000 °C (20 min), the photoresponse intensity slightly varies while a drastic (of about 20 times) decrease in the leakage currents is observed.

As for Si10, the behavior of the leakage currents can be considered only for mesa-etched diodes (currents decrease by more than a factor of 80).

In Figs. 4–6, the IR photosensitivity spectra for three types of the structures are shown. Si70 spectra have been studied most comprehensively to determine a dose optimal for the photoresponse in the range of 1×10^{14}–1×10^{15} cm^{-2}.

From Fig. 4 it is obvious that the photosensitivity increases up 6×10^{14} cm^{-2} and then decreases for higher doses. All the spectra exhibit the main maximum corresponding to the wavelength of 1.83 μm (0.68 eV)

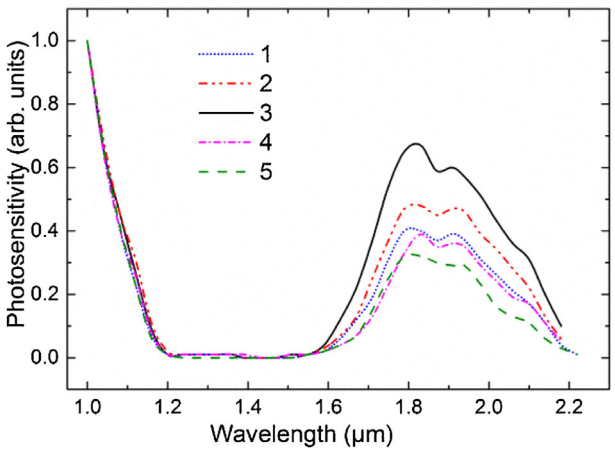

Figure 4 Relative photosensitivity spectra of the p-n diode (Si70) for different doses: 1–1×10^{14}; 2–4×10^{14}; 3–6×10^{14}; 4–8×10^{14}; 5–1×10^{15} cm^{-2}.

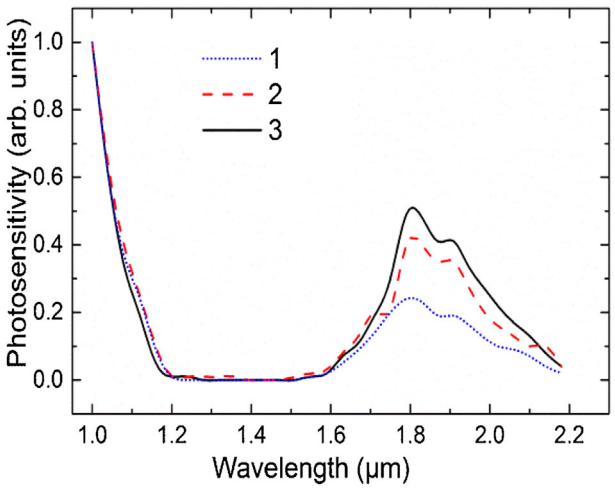

Figure 5 Relative photosensitivity spectra of the p-n diode (Si10) for different doses: 1–1×10^{14}; 2–4×10^{14}; 3–6×10^{14} cm^{-2}.

and a less pronounced (smoothed) maximum at 1.92 μm (0.65 eV).

For low resistance silicon (Si10) the same picture is qualitatively observed (Fig. 5): increasing the dose from 1×10^{14}–6×10^{14} cm^{-2} the photoresponse intensity increases. However, in this case, it is lower for each fixed dose compared to Fig. 4. The main peak is slightly shifted toward higher energies of 1.8 μm (0.69 eV) and the smoothed peak has a maximum at 1.91 μm (0.65 eV).

In Fig. 6, a photosensitivity spectrum of the SOI p-n diode is shown. In this case, the character of the dependence differs markedly from the two previous ones: the spectrum is extended, the main maximum is observed at 1.75 μm (0.72 eV), and the second maximum is shifted to the wavelength of 2.04 μm (0.61 eV).

Figure 7 shows the influence of the pulse photon annealing on the photoresponse of p–n diodes (Si10) B^+ implanted with a dose of 1×10^{14} cm^{-2}

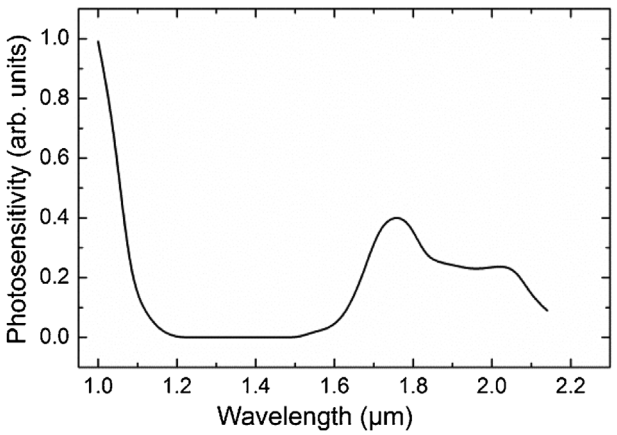

Figure 6 Relative photosensitivity spectra of the p-n diodes on SOI for the dose of 4×10^{14} cm^{-2}.

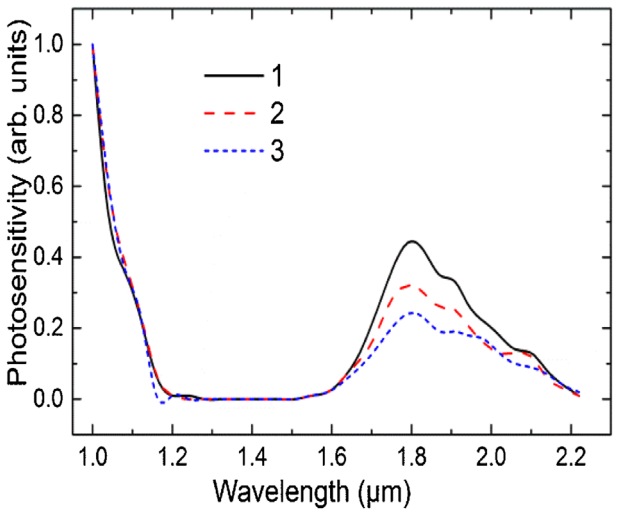

Figure 7 Relative photosensitivity spectra of the p–n diodes (Si10) for different thermal treatment conditions (dose 1×10^{14} cm^{-2}): 1–photon annealing at seven 3-s pulses; 2 – at three 3-s pulses; 3 – in the stationary conditions.

It is seen from the figure that the photon impact is more effective, though the annealing temperatures are nearly the same (900 °C). This concept needs further investigation.

Figure 8 demonstrates the integral photosensitivity spectrum of the p–n diode (Si70) where, using a filter system, separate spectral regions within 0.2–4.1 μm are singled out.

The illumination of the sample with the wave packet allows one to assess the general picture of the photoresponse within the wide range, and particularly the percentage ratio between the photosensitivity in different wavelength subranges and the entire spectrum illumination. For this implantation dose, the main percentage of the photoresponse is observed within 750–1200 nm, whereas in the SWIR this value is about 6% and may reach 9%.

Figure 9 shows the photosensitivity vs. the wavelength due to the B^+ implantation with the dose of 1×10^{13} cm^{-2}

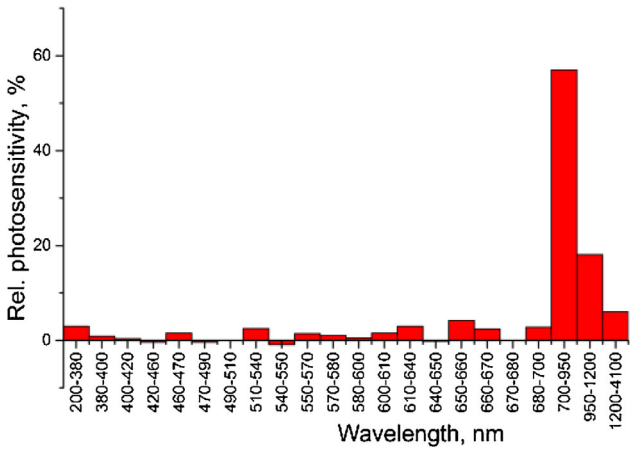

Figure 8 Spectral dependence of the integral relative photosensitivity for the p–n diode (Si70) and the dose of $1 \cdot 10^{14}$ cm^{-2}.

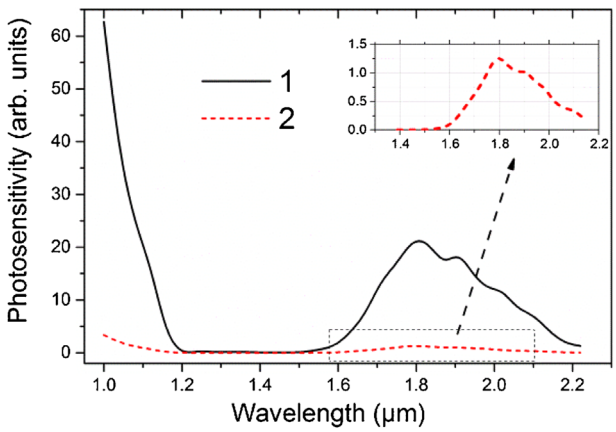

Figure 9 Relative photosensitivity spectra for the Si70 samples implanted with a dose of 1×10^{13} cm^{-2}: 1 – the substrate surface is not etched; 2 – the surface etched to a depth of about 1 μm; in the upper right corner the dependence 2 in the enlarged scale is given.

into the starting material (1) and after the etching of the wafer surface layer to a depth of about 1 μm (2).

As can be seen from the figure, after the etching of the damaged layer the photoresponse intensity decreases by 20 times, and the main maximum is distinctly less pronounced. The sample with the etched layer behaves in accordance with the stated existence of a threshold dose of 1×10^{14} cm^{-2} to form extended defects.

In the previous article [2], it was shown that in the starting material as well as in the material annealed up to 900° and 1000 °C or B^+ implanted without annealing within the SEM sensitivity range, only silicon is detected. Here, more comprehensive data on the detection of carbon and oxygen impurities at the depth of 1 μm in Si70 samples at different doses of implantation and annealing temperatures (900°C, 1000°C) are given (Fig. 10).

The detection of C and O after implantation and annealing indicates the gettering of these impurities to the surface. From these figures it can be concluded in the first

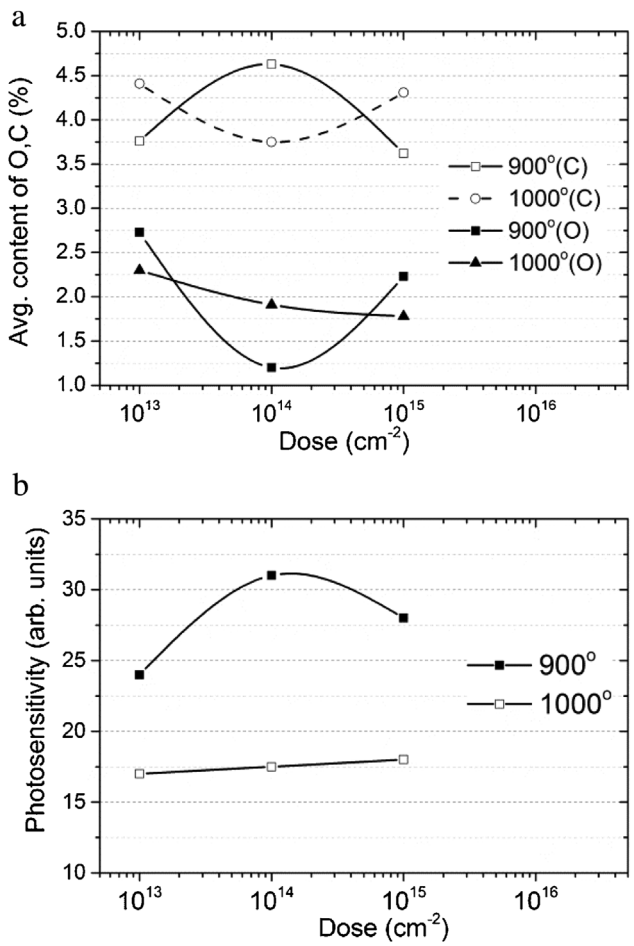

Figure 10 Dose and annealing temperature dependences of: a – carbon and oxygen content; b – relative integrate photosensitivity.

approximation that oxygen has the most critical effect on the formation of defects responsible for the photosensitivity; the lower its content, the higher the photoresponse at both annealing temperatures.

The C content, though higher than O in our case, appears to be less critical.

In interpreting the results it seems appropriate to rely on the following points.

1. When interpreting *the photosensitivity spectra* of p–n Si structures (Figs.4–7) it should be taken into account that the IR spectra cannot be associated with a change in the band structure of the implanted region: first, our previous results [4] demonstrated insignificant variations in the crystal lattice parameters determined by X-ray diffractometry; secondly, no pronounced increase in the intensity of the integral photosensivity due to the shift of the self-absorption edge is observed (Fig. 8). Under the used implantation and annealing conditions, the optical properties of the material can be explained by the content of extended defect, including those which at all doses for Si70 and Si10 create deep levels with the activation energy of E_c-0.7 eV and E_c-0.65 eV in the bandgap. The corresponding maxima (main and smoothed) in the photosensitivity spectra are characterized by the different dose-dependent intensity. It is reasonable to assume that the photoresponse spectra are due to the two different types of defects with close activation energies. The increase in the photosensitivity intensity up to the dose of 6×10^{14} cm^{-2} is associated with the increase in the concentration of these defects. With further increasing dose up to 1×10^{15} cm^{-2} the concentration of the extended defects should increase. However, the decrease in the intensity indicates that the number of active defects decreases and new defects occur that do not affect the optical properties of the material.
   For the SOI structures, the shape of the curve and the activation energy values are somewhat shifted. The share of the photosensitivity in the SWIR is 6–9% of the integrated photosensitivity in the range of 200–4100 nm. According to the numerous literature data, it is reasonable to assume that under these implantation and annealing conditions these extended defects are dislocation loops.
2. For a more comprehensive explanation of the observed phenomena we thought it reasonable to use the concept of *the long-range effect* for ion implanted semiconductors [14]. According to this model, we can distinguish two qualitatively different regions of the subsurface layer, modified by ion implantation. In the first region, the alloyed surface layer is located directly under the irradiated target surface and has a thickness of the order of the ion range. The second region is the sublayer which is characterized by an abnormally deep penetration of defects induced by ion irradiation.
   The fact that the photoresponse intensity in high-resistance samples (Si70) is higher than in the low-resistance case (Si10) is explained by the different p–n depths (*cf.* Figs. 4 and 5).
3. The observed interesting fact of a drastic increase in the *leakage currents* with an increasing dose from 6×10^{14}–1×10^{15} cm^{-2} (Fig. 3) can be explained as follows. At high doses, a change in the process of defect formation is assumed, which determines the formation of new defects a part of which leads to generation-recombination processes and hence affects the reverse current in the diode. According to Ref. [15], such defects may be dislocations.
4. *The damaged layer of the crystal lattice* in n-Si, extending from the surface to a depth of a few hundred nanometers [2, 3, 16], plays a decisive role in the complex processes of defect formation mechanism leading to the appearance of photosensitivity in p–n structures. In the present article, a direct experimental confirmation was found (Fig. 9) that during B^+ implantation in n-Si the formation of defects responsible for IR photosensitivity in p–n diodes occurs in the damaged layer of the original n-Si.

5. The understanding of the defect formation mechanism becomes even more complicated due to the observed correlation between the content *of carbon and oxygen impurities* in the surface layer and the IR photoresponse at different doses and annealing regimes (Fig. 10). At this stage, we can only assume that the effect of oxygen on the defects responsible for the photosensitivity is much stronger than that of carbon. This assumption is in agreement with the data of [17], where it is shown that the presence of O in the silicon wafers deteriorates the photosensitivity of devices.
6. Using the damaged layer in the starting material, it is possible to realize the controllable optical properties of p–n structures and propose this process as an innovative approach to the development of *SWIR array photodetectors*. In this respect, high-resistance n-Si samples implanted with a dose of B^+ 6×10^{14} cm^{-2} and annealed at 900 °C (20 min) may find practical application. These structures can be used for SWIR pixel arrays. On the basis of SOI structures a quasi-planar array can be developed, especially for those cases where a relatively weak output signal is "compensated" by low leakage currents.

4 Conclusions The results of the investigation can be summarized as follows: The optical and electrical characteristics of p–n diodes based on monocrystalline n-Si (wafers with different resistivity and SOI) obtained by B^+ ion implantation with various doses of 1×10^{14}–1×10^{15} cm^{-2}, the energy of acceleration of 50 keV, and annealed at 900 °C (20 min) have been investigated.

For wafers, the photosensitivity spectra exhibit in the range of 1.5–2.2 μm, two maxima – main and smoothed, with energies of 0.68–0.69 eV and 0.65 eV, respectively, the intensity of which depend on the dose and resistance of the material. For SOI, they are slightly shifted.

A qualitative mechanism of the observed effects is proposed which consists of the formation of extended defects with DL (E_c–0.7 eV and E_c–0.65 eV for Si70 and Si10; E_c–0.72 eV and E_c–0.61 eV for SOI) in the bandgap. According to the long-range effect model, these defects penetrate to the depth exceeding that of the p–n junction. Apparently, with an increasing dose from 1×10^{14}–6×10^{14} cm^{-2}, the concentration of electrically active defects increases. At higher doses, the concentration of these defects decreases, and new defects occur that do not affect the optical properties of the structure. It is reasonable to relate the drastic increase in the reverse current in the p–n diode at high doses to generation-recombination processes due to the appearance of new defects (e.g., dislocations).

The determining effect of the disturbed surface layer in monocrystalline n-Si on the structural, electrical and optical properties of the samples has been experimentally confirmed.

An interesting correlation between the content of C and O gettered to the sample surface due to B ion doping and the photoresponse at different doses and annealing temperatures has been found. This fact needs further investigation.

The experimental results as a whole can be considered quite reliable, since they are obtained on a large number of samples and are well reproducible.

According to the results of the investigation, an innovative approach to manufacturing of IR array photodetectors, namely pixel-arrays based on high-resistance n-Si, and quasi-planar arrays based on SOI is emerging.

Acknowledgements We gratefully acknowledge M. Ksaverieva for the participation in measurements, and G. Kalandadze and L. Sanikidze for formation of ohmic contacts.

References

[1] V. N. Kotov, V. G. Klindukhov, and I. I. Cherepakhin, Nano i Microsistemnaya Tekhnika **3**, 8 (2000).
[2] N. Khuchua, M. Tigishvili, R. Melkadze, N. Dolidze, N. Gapishvili, Z. Jibuti, G. Dovbeshko, and V. Romanyuk, Solid State Phenomena **242**, 374 (2016).
[3] N. P. Khuchua, N. D. Dolidze, N. G. Gapishvili, R. G. Gulyaev, Z. V. Jibuti, R. G. Melkadze, and M. G. Tigishvili, Nanotechnol. Percept. **10**(2), 288 (2014).
[4] M. G. Tigishvili, N. G. Gapishvili, R. G. Gulyaev, Z. V. Jibuti, N. D. Dolidze, N. P. Khucua, and R. G. Melkadze, Georg. Eng. News **68**, 75 (2013).
[5] N. A. Sobolev, A. M. Emelianov, E. I. Shek, and V. I. Vdovin, Fizika Tverd.Tela **46**, 39 (2004).
[6] M. A. Lourenco, M. Milosavljevic, G. Shao, R. M. Gwilliam, and K. P. Homewood, Thin Solid Films **504**, 36 (2006).
[7] M. Casalino, Int. J. Opt. Appl. **2**(I), 1 (2012).
[8] Ph. Ph. Komarov, M. Jadan, P. I. Gaiduk, A. R. Cheladinski, V. Yu. Yavid, P. V. Zhukovski, Ya. Partika, and P. Vengerek, Fizika I Khimia Obrabotki Materialov **4**, 33 (2004).
[9] V. I. Plebanovich, A. I. Belous, A. R. Cheladinski, and V. B. Ojaev, Fizika Tverd. Tela **50**, 1378 (2008).
[10] R. J. Schrentelkamp, J. S. Custer, J. R. Liefting, W. X. Lu, and F. W. Saris, Mater. Sci. Rep. **6**, 275 (1991).
[11] S. Eichler, J. Gebauer, F. Boerner, A. Polity, and R. Krause-Rehberg, Phys. Rev. B **56**, 1393 (1997).
[12] S. Libertino and A. L. Magna, Topics Appl. Phys. **116**, 147 (2010).
[13] A. R. Cheladinski and Ph. Ph. Komarov, Uspekhi Fizicheskikh Nauk **173**, 813 (2003).
[14] N. P. Aparina, M. I. Guseva, B. N. Kolbasov, S. N. Korshunov, A. N. Mansurova, Yu. V. Martynenko, I. V. Borovitskaya, and L. I. Ivanov, Voprosi atomnoy nauki I tekhniki **3**, 18 (2007).
[15] R. H. Glaense and A. G. Jordan, Phil. Mag. **18**, 717 (1968).
[16] A. N. Mikhajlov, A. I. Belov, D. S. Korolyev, A. O. Timofeeva, B. K. Vasilyev, A. I. Bobrov, D. A. Pavlov, D. I. Tetelbaum, and E. B. Shek, Physika i tekhnika poluprovodnikov **48**, 212 (2014).
[17] V. I. Blynski, O. A. Bozhatkin, E. S. Holub, A. M. Lemeshevskaya, and S. V. Shvedov, J. Appl. Spectr. **77**, 478 (2010).

